Biophysical Chemistry 154 (2011) 1–7

Contents lists available at ScienceDirect

Biophysical Chemistry

journal homepage: http://www.elsevier.com/locate/biophyschem

Hydration properties of adenosine phosphate series as studied by microwave dielectric spectroscopy

George Mogami [a], Tetsuichi Wazawa [a], Nobuyuki Morimoto [a], Takao Kodama [b], Makoto Suzuki [a,*]

[a] Laboratory of Biomaterials Physical Chemistry, Department of Materials Processing, Graduate School of Engineering, Tohoku University, CREST/JST, 6-6-02 Aoba, Aramaki-aza, Aoba-Ku, Sendai, Miyagi 980-8579, Japan
[b] Immunology Frontier Research Center, Osaka University, 3-1 Yamada-Oka, Suita, Osaka 565-0871, Japan

ARTICLE INFO

Article history:
Received 10 October 2010
Received in revised form 13 November 2010
Accepted 21 November 2010
Available online 29 November 2010

Keywords:
Dielectric dispersion
Debye relaxation
Adenosine triphosphate
Orthophosphate
Hydration number
Hyper-mobile water

ABSTRACT

Hydration properties of adenine nucleotides and orthophosphate (Pi) in aqueous solutions adjusted to pH = 8 with NaOH were studied by high-resolution microwave dielectric relaxation (DR) spectroscopy at 20 °C. The dielectric spectra were analyzed using a mixture theory combined with a least-squares Debye decomposition method. Solutions of Pi and adenine nucleotides showed qualitatively similar dielectric properties described by two Debye components. One component was characterized by a relaxation frequency (f_c = 18.8–19.7 GHz) significantly higher than that of bulk water (17 GHz) and the other by a much lower f_c (6.4–7.6 GHz), which are referred to here as hyper-mobile water and constrained water, respectively. By contrast, a hydration shell of only the latter type was found for adenosine (f_c ~ 6.7 GHz). The present results indicate that phosphoryl groups are mostly responsible for affecting the structure of the water surrounding the adenine nucleotides by forming one constrained water layer and an additional three or four layers of hyper-mobile water.

1. Introduction

ATP is the principal energy carrier in living cells. Its hydrolysis into ADP and inorganic phosphate (Pi) is accompanied by a large negative change of the Gibbs energy ($\Delta_{hyd}G$) at physiological pH. This is also the case for some other phosphate esters as well. Owing to this energetic feature, these phosphates are referred to as energy-rich phosphates [1].

Various bond energy-based descriptions have been proposed to explain the large negative $\Delta_{hyd}G$ for such phosphates [2]. However, even when elaborated by advanced quantum-level calculations, no such hypothesis has satisfactorily explained the observed energetics of hydrolysis. As suggested by George et al. as early as 1970 [3], the most probable reason for this is that the solvent water has either been ignored or at best regarded as a continuous dielectric for the purpose of calculations, despite the fact that hydrolysis occurs in the aqueous phase. In recent years, several attempts have been made to calculate the $\Delta_{hyd}G$ by considering energetic changes induced by solute–solvent interactions, but none of them has so far succeeded [4–7]. This indicates that our understanding of solute–solvent interactions is insufficient for reaction species involved in the hydrolysis of energy-rich phosphates. This problem is in part ascribed to the lack of experimental knowledge of the hydration state of these phosphates, which is invaluable to verify theoretical calculations and create models for theoretical consideration. In light of the importance of such information, we have attempted to characterize the hydration states of reaction species involved in ATP hydrolysis.

Here, we employ dielectric relaxation (DR) spectroscopy, which measures the electric response of a material to an oscillating electric field of small amplitude. The frequency dependence of the complex dielectric permittivity of a sample provides detailed information on dynamic processes involving the polarizable components. In the case of aqueous solutions, we can obtain information about the cooperative rotational motion of water molecules, ion-cloud relaxation, ion-pair rotation, and intra-molecular structural relaxation of solutes. With DR spectroscopy, we previously characterized the hydration states of various proteins [8–12], sodium halide salts [13], and cytochrome *c* upon acid-induced unfolding [14] in aqueous solutions, which provide an excellent foundation for our present approach.

Here, we measured DR spectra of aqueous solutions of ATP, ADP, and AMP (together referred to as adenine nucleotides) and Pi at pH 8.0, where the major ionic species were ATP^{4-}, ADP^{3-}, AMP^{2-}, and HPO_4^{2-} with Na^+ as the counter ion in respective solutions. Concentrations of all solutions were dilute enough to prevent adenine nucleotides from self-association [15], ensuring their monodispersed state. The spectra were then analyzed to obtain the hydration properties of ATP and all other chemical species involved in the hydrolysis reaction. The results are discussed by focusing on the role of the phosphoryl group in the hydration of adenine nucleotides.

* Corresponding author. Tel./fax: +81 22 795 7303.
E-mail address: msuzuki@material.tohoku.ac.jp (M. Suzuki).

0301-4622/$ – see front matter © 2010 Elsevier B.V. All rights reserved.
doi:10.1016/j.bpc.2010.11.006

2. Materials and methods

2.1. Preparation of solutions

All reagents at the highest purity commercially available were used as supplied. Sources were Oriental Yeast Co. (Tokyo, Japan) for disodium salts of adenine nucleotides (ATP, ADP, and AMP; their manufacturer-guaranteed purities were all >95%) and Wako Pure Chemical Industries (Osaka, Japan) for adenosine (purity >98%), concentrated phosphoric acid (85% (w/w)) and 1 M sodium hydroxide solution for volumetric analysis (1 M NaOH).

Milli-Q water (Millipore Co., Billerica, MA) was used to prepare all the solutions for dielectric spectroscopy. The solutions of adenine nucleotides were freshly prepared, and the Pi solutions were those of diluted phosphoric acid. These solutions were adjusted to pH 8.0 ± 0.05 by 1 M NaOH. At this pH, completely H^+-dissociated forms (ATP^{4-}, ADP^{3-}, and AMP^{2-}) and HPO_4^{2-} were the major ionic species in solutions of adenine nucleotides and Pi, respectively, and the common counter ion was Na^+ (Table 1 and Supplementary Fig. S1). The adenosine solution was prepared by dissolving the solid material, which was left standing overnight and then passed through a membrane filter with a pore diameter of 0.22 μm and used without pH adjustment. Concentrations of adenosine and adenine nucleotides were determined from absorbance at 260 nm with a molar absorbance coefficient (L mol^{-1} cm^{-1}) of 15.1×10^3 and 15.4×10^3, respectively. Partial specific volumes (ν_B) were calculated from the solution densities measured in an Anton-Paar DMA-58 density meter (Graz, Austria). Table 1 lists the ionic species in each solution measured and analyzed in the present study. The monomer ratios of adenine nucleotides and adenosine are also given in Table 1, indicating that all the solutions other than the adenosine solution can be assumed to be monodispersed.

2.2. Dielectric spectroscopy: experimental

All measurements were carried out using a microwave network analyzer (PNA8364B-85070E, Agilent, Santa Clara, CA) with an open-end coaxial flat surface probe (high temperature type, 19 mm diameter, electric length ≈ 45 mm, Agilent) immersed in a conically shaped glass cell (total volume of 3.2 mL) containing a sample solution that had been degassed before loading. The cell was held at 20.00 ± 0.01 °C by a temperature-controlled circulator (NESLAB RTE-17, Thermo Fisher Scientific, Waltham, MA). The whole measuring system was placed in an air-conditioned room maintained at 20 ± 1 °C. The probe calibration was performed by three separate runs: open-circuited to the air, short-circuited with mercury and in contact with pure water. DR spectra were recorded for the frequency range of 0.2–26 GHz (301 frequency points in log-scale) as previously described [13]. In short, the DR spectra of the water reference ($\varepsilon^*_w(f)$) and a sample solution ($\varepsilon^*_{ap}(f)$) were measured alternately four to eight times to reduce the effect of the machine drift over a period of two hours for a given solution. After DR measurements, solutions of adenine nucleotides were analyzed using a 626LC HPLC system (Waters, Milford, MA, USA) with a Fractogel EMD TMAE (S) strong anion exchanger (φ10 × 100 mm, 116887, Merck). The mobile phase was a gradient from water to 0.25 M phosphate at pH 7.3.

2.3. Dielectric spectroscopy: data analysis

All the spectra thus obtained and subjected to the analysis are shown in Fig. 1A. For all solutions, the difference between a sample and the water reference spectra was very small but systematic (Fig. 1B). The difference DR spectrum for each pair was calculated using Eq. (1).

$$\Delta\varepsilon^*(f) = \Delta\varepsilon'(f) - i\Delta\varepsilon''(f) = \varepsilon^*_{ap}(f) - \varepsilon^*_w(f) - i\frac{\Delta\sigma}{2\pi f\varepsilon_0}, \quad (1)$$

where $\Delta\sigma$ is the difference of static electrical conductivity between a given sample at a specified concentration and pure water. The value of $\Delta\sigma$ was initially adjusted so as to give $\Delta\varepsilon''(0.2\ \mathrm{GHz}) = 1$ and eventually determined by iterative parameter fitting, as described in the following section. The difference spectra obtained from Eq. (1) were then averaged and smoothed to eliminate the resonance noise induced by the probe over its whole length at a frequency range of 2–6 GHz. The smoothed spectral curves were determined using the third- to fifth-order polynomial functions of $\log(f)$, as shown in Fig. 1B. The standard errors of $\Delta\varepsilon'(f)$ and $\Delta\varepsilon''(f)$ over four to eight separate experiments were 0.01 or less over 1–26 GHz. Smoothed spectra $\varepsilon^*_{ap}(f)$ were rebuilt by summing up $\Delta\varepsilon^*(f)$ and $\varepsilon^*_w(f)$.

An independent experiment was carried out to check the accuracy of the present measurements using aqueous solution of ethanol (8 mol%) as a standard sample (Fig. S3 of Supplementary material). As can be seen, the spectral curves from our measurements agreed well with those reported previously by different laboratories [16,17] over a frequency range covered by our instrument. In addition, eight separate measurements were highly reproducible. Small standard errors accompanying observed values in Table 2 were reflections of this high precision technique, which assured to analyze the small differences in dielectric spectra obtained in this study as follows.

Using Hanai mixture theory [18], the dielectric spectrum $\varepsilon^*_{ap}(f)$ of a sample solution was mathematically separated into two components, the bulk water $\varepsilon^*_w(f)$ and the solute with a water shell $\varepsilon^*_q(f)$ at an arbitrary volume fraction ϕ (v < ϕ < 1), as given by Eq. (2),

$$\varepsilon^*_q = \left\{\varepsilon^*_{ap} - (1-\phi)\left(\frac{\varepsilon^*_{ap}}{\varepsilon^*_w}\right)^{\frac{1}{3}}\varepsilon^*_w\right\} \Big/ \left\{1-(1-\phi)\left(\frac{\varepsilon^*_{ap}}{\varepsilon^*_w}\right)^{\frac{1}{3}}\right\}. \quad (2)$$

Table 1
Specification of solutions measured in the present study.

Solutions	Concentration (mM)	pH	Na^+ concentration (mM)	Ionic species[c]	Monomer molar ratio[d]
ATP	7.36[a]	8.00	28.9	ATP^{4-}, 0.92; $HATP^{3-}$, 0.08	0.98
	12.7[a]	7.95	49.7	ATP^{4-}, 0.91; $HATP^{3-}$, 0.09	0.97
	29.6[a]	7.99	116.0	ATP^{4-}, 0.92; $HATP^{3-}$, 0.08	0.92
ADP	15.7[a]	8.03	46.0	ADP^{3-}, 0.93; $HADP^{2-}$, 0.07	0.94
	27.5[a]	7.99	80.6	ADP^{3-}, 0.93; $HADP^{2-}$, 0.07	0.90
AMP	13.0[a]	8.00	25.6	AMP^{2-}, 0.97; $HAMP^{-}$, 0.03	0.95
	30.3[a]	8.01	59.7	AMP^{2-}, 0.97; $HAMP^{-}$, 0.03	0.87
Pi	14.7[b]	7.97	28.5	HPO_4^{2-}; 0.94 $H_2PO_4^-$, 0.06	–
	19.6[b]	8.00	38.0	HPO_4^{2-}; 0.94 $H_2PO_4^-$, 0.06	–
	31.0[b]	8.05	60.5	HPO_4^{2-}; 0.95 $H_2PO_4^-$, 0.05	–
Adenosine	5.8[a]	9	0	Negligible (6 < pH < 10)	0.83
	8.8[a]	9	0	Negligible (6 < pH < 10)	0.74

[a] Determined by spectrophotometry.
[b] Determined by titration.
[c] Calculated with p*K*a values given in Refs. [31,33].
[d] Calculated with the self-association constants, K_{SA} values in Ref. [15](ATP^{4-}, 1.3; ADP^{3-}, 1.8; AMP^{2-}, 2.1; and adenosine, 15).

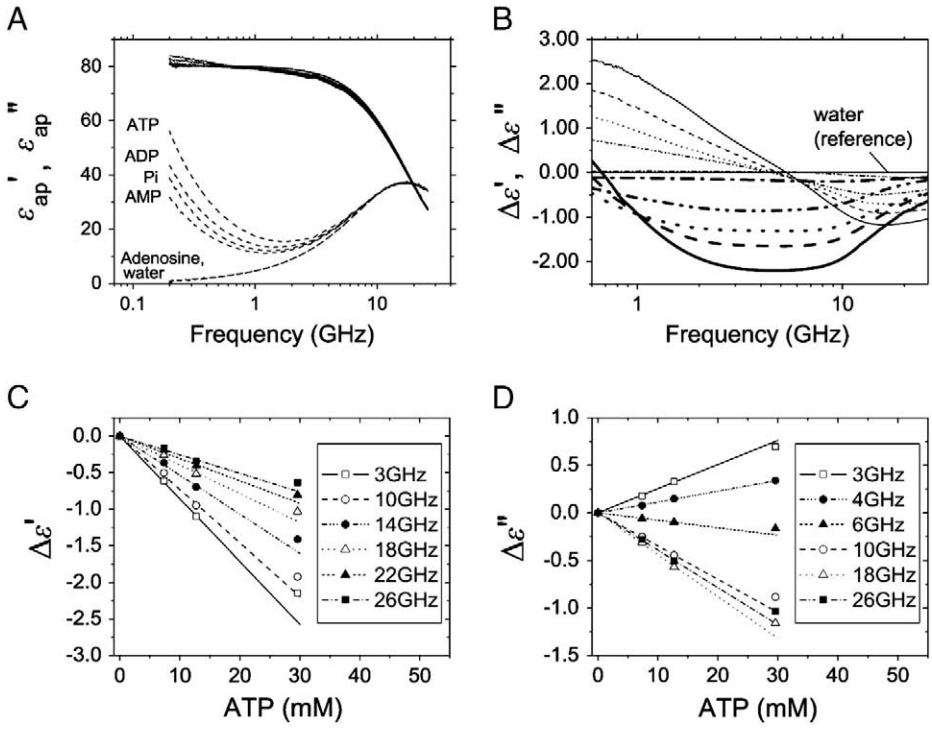

Fig. 1. Dielectric spectra of aqueous solutions of ATP, ADP, AMP, adenosine, and Pi at 20.00 °C. (A) Dielectric spectra $\varepsilon^*_{ap}(f)$. Solid and dashed lines indicate ε'_{ap} and ε''_{ap}, respectively. (B) Difference dielectric spectra. Difference dielectric spectra ($\Delta\varepsilon' = \varepsilon'_{ap} - \varepsilon'_w$, thick line; $\Delta\varepsilon'' = \varepsilon''_{ap} - \varepsilon''_w$, thin line) were averaged over n experiments and smoothed for ATP ($n = 4$, solid line), ADP ($n = 6$, dashed line), AMP ($n = 4$, dotted line), adenosine ($n = 5$, chain line), and Pi ($n = 8$, two-dot chain line). In all cases, error bars are much smaller than the symbol sizes of $\Delta\varepsilon'$ and $\Delta\varepsilon''$. (C) Concentration dependence of $\Delta\varepsilon'$ for ATP. (D) Concentration dependence of $\Delta\varepsilon''$ for ATP.

v is the volume fraction of a given solute calculated by $v = cM_w v_B/1000$, where M_w, c, and v_B are the molar mass in g/mol, the molar concentration of solute molecule in mol/L, and the partial specific volume of solute in mL/g, respectively. In the frequency range of 3–26 GHz, $\varepsilon^*_q(f)$ can be decomposed into a series of Debye functions and the bulk water component ($f_{cw} \approx 17$ GHz; $\delta_w \approx 75.0$ at 20 °C) by Eq.(3):

$$\varepsilon^*_q(f) \cong \varepsilon^*_{q,sim}(f) = \varepsilon_{q,\infty} + \alpha\left(\varepsilon^*_w(f) - \varepsilon_{w,\infty}\right) + \sum_{j=1}^{m} \frac{\delta_j}{1 + i\left(f/f_{cj}\right)}, \quad (3)$$

where $\varepsilon_{q,\infty}$ and $\varepsilon_{w,\infty}$ are the dielectric constant of the solute in the high-frequency limit and that of water, respectively, α is the fraction of water contribution, and f_{cj} and δ_j are DR frequency and DR amplitude of the j-th Debye component, respectively. Using the value of $\varepsilon_{w,\infty} = 5.4$ at 20 °C [19,20], $\varepsilon_{q,\infty}$ was set to 5.0 based on the following considerations. Considering the static dielectric permittivity of solutes ~3.1, derived from electronic polarizabilities given in Ref [21], the value of $\varepsilon_{q,\infty}$ was calculated to lie between 5.0 and 5.4 based on Wagner theory [22] in the present samples. This indefiniteness has only a small effect on the

Table 2
DR parameters of the hydrated ATP, ADP, AMP, adenosine, and Pi in water.

A. Dielectric properties of hydrated solutes

Solutions[a]	f_{c3} (GHz)[b]	δ_3/c (M^{-1})[b]	$\Delta\sigma/c$ (S m^{-1} M^{-1})	f_{c2} (GHz)	δ_2	f_{c1} (GHz)	δ_1	ϕ_B/c (M^{-1})
ATP	0.270 ± 0.017	7610 ± 30	24.9 ± 0.1	7.2 ± 0.4	8.3 ± 0.3	19.1 ± 0.2	55.9 ± 1.7	8.40 ± 1.18
ADP	0.259 ± 0.016	5050 ± 40	16.0 ± 0.1	7.7 ± 0.4	10.4 ± 0.6	19.2 ± 0.1	53.9 ± 0.9	5.26 ± 0.52
AMP	0.289 ± 0.018	2480 ± 30	12.4 ± 0.1	7.8 ± 0.5	11.1 ± 1.1	18.9 ± 0.2	53.9 ± 1.8	4.78 ± 0.53
Adenosine	0.87 ± 0.48	210 ± 50	0.3 ± 0.2	8.0 ± 1.0	38 ± 5	–	–	0.43 ± 0.06
Pi	0.410 ± 0.057	940 ± 10	13.5 ± 0.1	7.6 ± 0.4	10.2 ± 1.1	19.6 ± 0.4	55.8 ± 2.4	3.53 ± 0.61

B. Comparison of hydration numbers

Solutions	δ_2 (f_{c2} = 7.47 GHz)	δ_1 (f_{c1} = 18.92 GHz)	δ_w (f_{cw} = 17.0 GHz)	N_{total}[c]	N_2 (constrained)[d]	N_1 (hyper-mobile)[d]
ATP	6.41 ± 0.25	45.4 ± 1.7	16.0 ± 2.0	443 ± 20	48 ± 3	395 ± 17
ADP	5.22 ± 0.18	33.0 ± 0.8	32.1 ± 1.0	289 ± 9	35 ± 2	254 ± 8
AMP	4.60 ± 0.16	25.8 ± 1.1	40.9 ± 1.3	210 ± 12	28 ± 2	182 ± 10
Adenosine	1.08 ± 0.31	–	72.6 ± 0.2	11 ± 2	11 ± 2	–
Pi	3.55 ± 0.06	26.8 ± 0.4	42.5 ± 0.4	211 ± 4	22 ± 1	189 ± 3

A. Data are the mean ± SE from repeated measurements as explained in the text.
B. Values of δ_1, δ_2, and δ_w were obtained at $\phi/c = 11.0$ M^{-1}.
[a] Concentrations (mM) : ATP, 7.36; ADP, 15.7; AMP, 13.0; Adenosine, 5.8; and Pi, 31.0.
[b] Calculated by Eqs. (2) ~ (4) with $\phi_2 = 0.05$.
[c] Obtained at $\alpha = 0$.
[d] Calculated by Eq. (6) with $\delta_{1,0} = 66.8$ and $\delta_{2,0} = 77$. The resolution and accuracy of N_2 values for adenine nucleotides were estimated to be ~7% and ~20%, respectively.

parameters f_{cj} and δ_j if $\delta_j \gg 0.4$. Throughout this study, $\varepsilon'_q(f)$ in the frequency range of 3–26 GHz was successfully fitted with Eq. (3) for $m=2$ to determine the DR parameter set (f_{c1}, δ_1; f_{c2}, δ_2) and α. The ϕ value that gives $\alpha=0$ is defined as the volume fraction ϕ_B corresponding to the hydration boundary.

In the frequency range of 0.2–3 GHz, Eq. (3) could not simulate the experimental spectral curves; therefore, we adopted the second solute model $\varepsilon^*_{q2}(f)$ with a volume fraction ϕ_2 to simulate the spectra including imaginary parts below 3 GHz. The model can simulate a cationic cloud motion around a negatively charged phosphate moiety, or a reorientation motion of solute dipole, or their combination responding to the ac electric field

$$\varepsilon^*_{q2}(f) = \varepsilon^*_w(f) + \frac{\delta_3}{1 + i(f/f_{c3})}. \quad (4)$$

When $f \gg f_{c3}$, $\varepsilon^*_{q2}(f)$ approaches $\varepsilon^*_w(f)$. Therefore, if $f_{c3} \ll 3$ GHz, it hardly affects the spectral curves in the range of 3–26 GHz. By mixing the second solute model of Eq. (4) with a fixed value ϕ_2 (e.g., $\phi_2=0.05$, which value hardly affects the DR parameter set (f_{c1}, δ_1; f_{c2}, δ_2) and ϕ_B as discussed in Section 3.2) into the spectrum $\varepsilon^*_{ap}(f)$ represented by Eqs. (2) and (3), the parameters f_{c3}, δ_3, and σ were determined by fitting the experimental spectral curves below 3 GHz. The calculation steps using Eqs. (3) and (4) in order was repeated until self-consistency was satisfied, and this resulted in a uniquely determined parameter set (f_{c1}, δ_1; f_{c2}, δ_2; f_{c3}, δ_3; and ϕ_B, $\Delta\sigma$). Here it is noted that δ_3 and $\Delta\sigma$ are thought to be proportional to the solute concentration c based on the second solute model.

Once ϕ_B was determined, the hydration number could be calculated with the volume fraction of hydrated solute by Eq. (5):

$$N_{total} = \frac{55.6(\phi_B - v)}{c}, \quad (5)$$

where 55.6 is the molar concentration of bulk water.

3. Results and discussion

3.1. Proportionality of $\Delta\varepsilon^*(f)$ to solute concentration

First of all, we confirmed by post-measurement analysis of sample solutions by HPLC that no detectable hydrolysis occurred to ATP or ADP during the DR measurements. The difference spectra for all solutions are shown in Fig. 1B. For all sample solutions of adenine nucleotides in the frequency range of 3–26 GHz, the standard errors were less than 0.01 for each solution. In Fig. 1C and D, $\Delta\varepsilon'$ and $\Delta\varepsilon''$ of the ATP solution at several sampled frequencies are plotted as a function of the solute concentration c, indicating that below 12 mM, both parameters are proportional to c within the experimental error. Similar proportional relationships were found for ADP, AMP, and Pi below 15 mM (see Supplementary Fig. S2). These results justify adopting Hanai mixture theory for monodispersed systems in the present analysis.

3.2. Dielectric parameters for hydrated solutes

At ϕ values decreasing stepwise from 0.10 to 0.02 with $\Delta\phi=-0.001$, the dielectric spectra of solute ions with a water shell $\varepsilon^*_q(f)$ were calculated from Eq. (2). The $\varepsilon'_q(f)$ curves above 3 GHz for adenosine, adenine nucleotides, and Pi were simulated by three Debye components within experimental error. A best-fit parameter set (f_{c1}, δ_1; f_{c2}, δ_2; f_{c3}, δ_3; and α, $\Delta\sigma$) was determined at each step of ϕ for the sample spectra. By setting $\alpha=0$, the volume fraction for the hydration boundary ϕ_B was determined as shown in Fig. 2A and summarized in Table 2A. Fig. 2B–F shows the spectra $\varepsilon^*_q(f)$ of the hydrated solutes, which had different dielectric properties from those of bulk water. As shown in Fig. 2A, variation of f_{c1}, δ_1, f_{c2}, and δ_2 with decreasing ϕ was very small in contrast with a marked decrease in α. This indicates that bulk water with f_{cw} and both relaxation components of f_{c1} and f_{c2} do exist. As for the effect of a low frequency relaxation component centered at ~0.3 GHz on the parameters of the higher frequency relaxation components, the values of f_{c1}, δ_1, f_{c2}, δ_2, and ϕ_B, which were determined by fitting the experimental curves between 3 and 26 GHz, were not sensitive to the ϕ_2 value. Thus, the differences of parameter values between $\phi_2=0.05$ and $\phi_2=0.2$ for f_{c1} (~19 GHz), δ_1, f_{c2} (~7 GHz), δ_2, and ϕ_B are 0.05%, 0.14%, 1.8%, 0.015%, and 0.27%, respectively. These values are much smaller than the corresponding standard errors given over 4–8 experiments for each condition shown in Table 2. In addition, the difference of the low relaxation frequency f_{c3} ~0.3 GHz between $\phi_2=0.05$ and $\phi_2=0.2$ was 6.2%. One reason for these small deviations is that δ_3 inversely correlates with ϕ_2. Thus, f_{c1}, δ_1, f_{c2}, δ_2, and ϕ_B, and even f_{c3} shown in Table 2 were uniquely determined.

3.3. Comparison of hydration shells of adenine nucleotides and adenosine

To compare the hydration shells of solutes, we adopted a fixed-ϕ and fixed-f_c analysis. As shown in Table 2A, all the tested samples other than adenosine gave similar values of f_{c1} and f_{c2}, thus allowing us to make a quantitative comparison of the dielectric properties of different hydrated solutes in the observed spherical region given by ϕ. Using the average values of f_{c2} (7.47 GHz$<f_{cw}$) and f_{c1} (18.92 GHz$>f_{cw}$), the values of ϕ_B were re-evaluated. The best fit DR amplitudes δ_1 for f_{c1} and δ_2 for f_{c2} were determined for adenine nucleotides, Pi and adenosine as shown in Table 2B. It should be noted that the adenosine solution was not monodispersed, containing 83% of the monomer form and 17% of the dimer form at 5.8 mM. This indicates that the observed hydration number of adenosine is underestimated by several percent with an assumption that the accessible surface area is proportional to the hydration number of the solute, where the hydration number of a dimer may be 10–20% less than twice the number of the monomer.

Fig. 3 shows that the total DR amplitudes for the fixed volume fraction were almost the same for ATP, ADP, AMP, and adenosine. It should be noted that with decreasing number of phosphoryl groups from ATP to adenosine, the value of $\delta_1+\delta_2$ decreased while δ_w increased. Moreover, since the solute volume fraction v was much smaller than ϕ_B, most of the matter in the region $\phi=\phi_B$ was water, thus indicating that the components of f_{c1} or f_{c2} and the bulk water component exchanged with each other. Thus, we denote the dispersion components f_{c2} and f_{c1} as 'constrained' water and 'hypermobile water' (HMW), respectively. An image of hydration structure of ATP is shown in Fig. 4.

Adopting a statistical mechanical approach, the formation mechanism of HMW around a charged large molecule was discussed elsewhere [23].

Compared to adenine nucleotides, adenosine was found to have less constrained water. The hydration property of AMP was similar to that of Pi. These results together indicate that the hydration properties of adenine nucleotides are mostly governed by the phosphoryl groups.

3.4. Total number of water molecules affected by solutes examined

The numbers presented here are not the hydration numbers commonly recognized as water molecules constrained by solutes, but the total numbers N_{total} of water molecules whose dielectric property is different from that of bulk water (determined by setting $\alpha=0$). Values of N_{total} for ATP, ADP, AMP, adenosine, and Pi with Na^+ as the counter ion are summarized in Table 2B.

3.5. Separation of hydration numbers into different Debye components

As shown in Table 2B, the total DR amplitudes δ_{total} ($=\delta_1+\delta_2+\delta_w$) for ATP, ADP, AMP, adenosine, and Pi were nearly invariable. Since

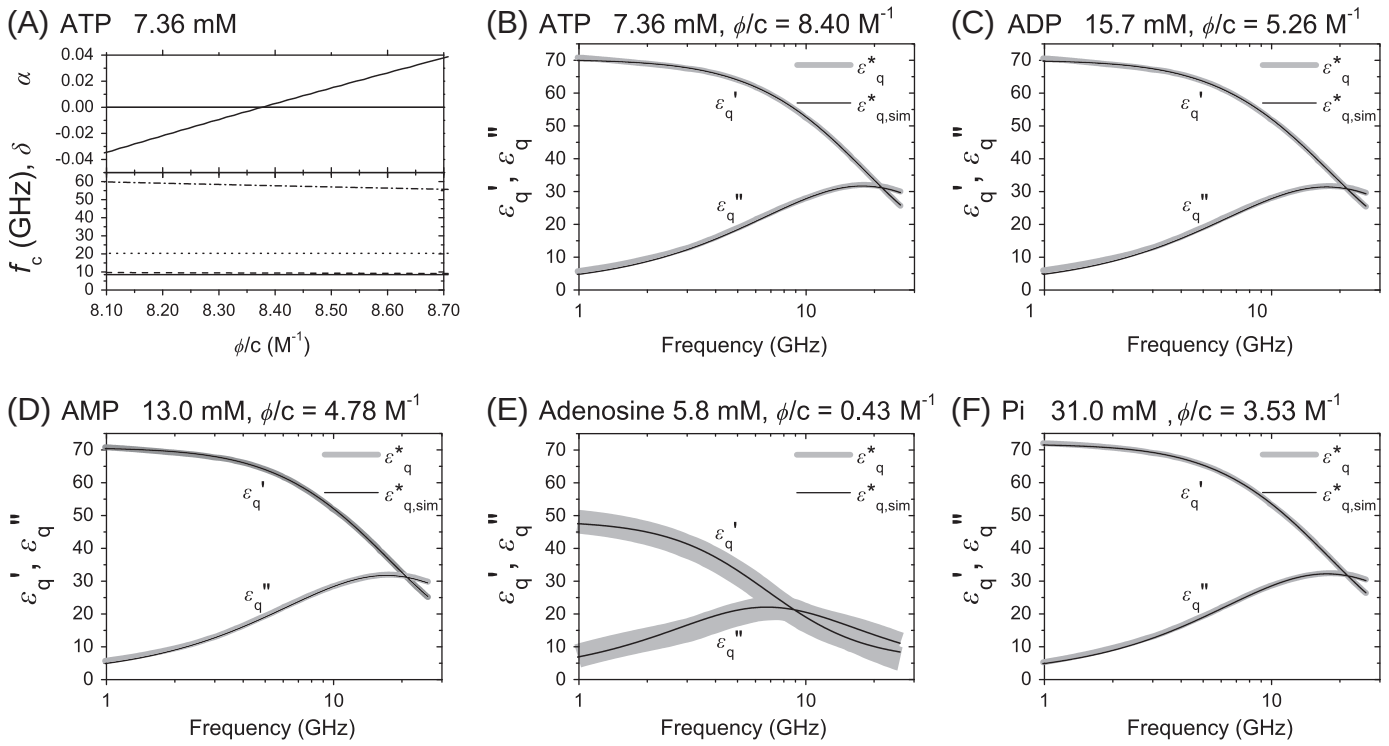

Fig. 2. Dielectric spectra of hydrated adenine nucleotides, and Pi. (A) Determination of the hydration boundary. The parameters (lower part) of the two Debye components and the fraction α (upper part) of the bulk water component were obtained by Eq. (3) as a function of ϕ/c. At the hydration boundary defined by $\alpha=0$, $\phi/c=\phi_B/c=8.40\ M^{-1}$ was determined for ATP. In lower part, solid, dashed, dotted, and chain lines indicate f_{c2}, δ_2, f_{c1}, and δ_1, respectively. Corresponding parameters for ADP, AMP, and Pi were determined (Table 2A). For adenosine, one Debye component could simulate $\varepsilon_q^*(f)$ and $\phi_B/c=0.43\ M^{-1}$. The corresponding dielectric spectrum for hydrated ATP at $\alpha=0$ is shown in (B) and those for hydrated ADP, AMP, adenosine, and Pi are shown in order of (C) to (F).

$\delta_{w,0}=75$ at 20 °C, the number of type-j water (1, hyper-mobile; 2, constrained), N_j, was calculated by Eq. (6),

$$N_1=\frac{\frac{\delta_1}{\delta_{1,0}}}{\frac{\delta_1}{\delta_{1,0}}+\frac{\delta_2}{\delta_{2,0}}}N_{total},\ N_2=\frac{\frac{\delta_2}{\delta_{2,0}}}{\frac{\delta_1}{\delta_{1,0}}+\frac{\delta_2}{\delta_{2,0}}}N_{total}, \tag{6}$$

where $\delta_{1,0}$ and $\delta_{2,0}$ are the DR amplitudes of pure components 1 and 2, respectively. An assumption used in this calculation is a simple proportional relationship between N_j and its DR amplitude δ_j. Taking into account that there exists no type-1 component around an adenosine molecule (see earlier discussion) and its dielectric permittivity of 3.1 based on Wagner theory [22] for a shelled sphere, the $\delta_{2,0}$ value for ATP was calculated to be 77 ± 13 from $\delta_2=37.7\pm5.2$ of the adenosine solution in Table 2A. Using the $\delta_{2,0}$ value, the $\delta_{1,0}$ value was then determined to be 66.8 ± 1.8 by Wagner theory [22] for double shelled sphere. The numbers N_1 and N_2 were then calculated as shown in Table 2B.

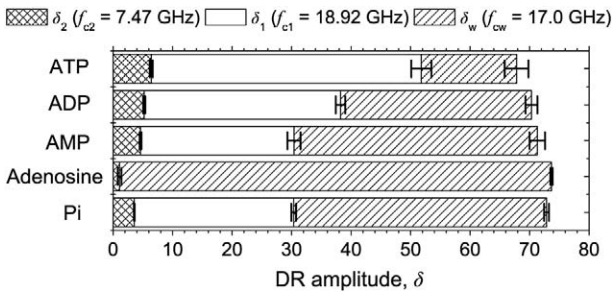

Fig. 3. DR amplitudes of the Debye components of ATP, ADP, AMP, adenosine, and Pi by the fixed-ϕ analysis ($\phi/c=11.0\ M^{-1}$), using $f_{c2}=7.47$ GHz for constrained water and $f_{c1}=18.92$ GHz for hyper-mobile water. The DR amplitudes of constrained water, hyper-mobile water and bulk water are indicated with cross-hatched, non-hatched, and diagonally hatched zones, respectively. Error bars indicate the standard errors over 4–8 measurements for each sample.

It should be noted that these numbers of constrained water for adenosine and ATP were larger than those of water molecules coordinated by their constituent atoms estimated by a recent MD study on Mg·ATP configuration in water [24]. It may be of interest in solution chemistry to investigate why such discrepancy arises.

3.6. Ion-pair effect on dielectric spectra

We have so far excluded the ion-pair effect in the assignment of f_{c1} and f_{c2} relaxation processes. The concentration employed in the present study was low (~15 mM), so that the ion-pair fraction would be very small in solution [25,26]. Moreover, even if there were ion pairs, their population should not be proportional to the solute concentration in the present concentration range. Accordingly, the volume fraction of ion pairs in solution would be much smaller than the observed values of ϕ_B. Thus, the effect of ion pairs on the present spectra can be neglected.

3.7. Effects of sodium ions on the dielectric properties of adenosine phosphates

In the present study, anionic species in all the solutions examined (except for the adenosine solution) were different but had Na^+ as their common counter ion. Hence, it is important to evaluate the effects of Na^+ on the observed hydration properties. A clue to this problem can be obtained from our previous study on NaCl solutions [13], where we detected only one Debye component of HMW in the range of 3–26 GHz, suggesting that no independent hydration shells with different DR frequencies exist around Na^+ or Cl^-. The same is the case for solutions of other halide salts of potassium as well as sodium

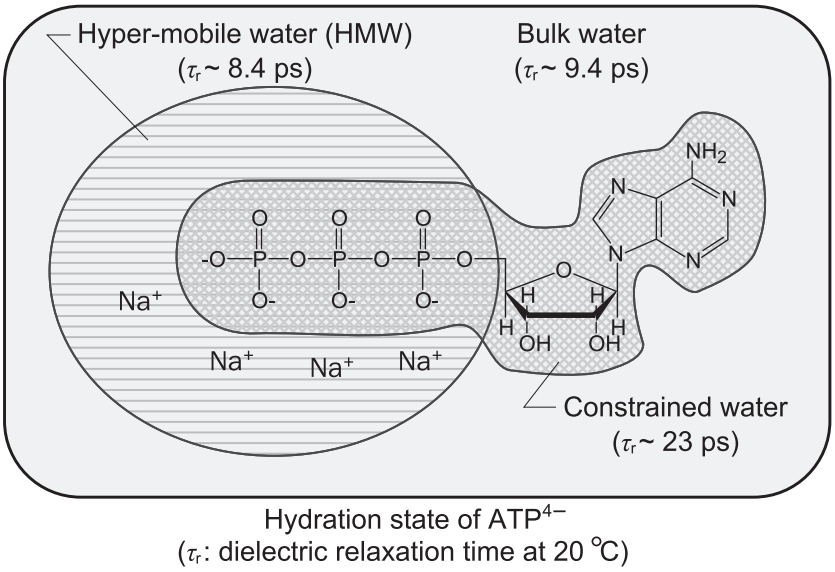

Fig. 4. An image of hydration structure of ATP revealed by the present study. The ATP anion (ATP^{4-}) coexists with charge-balancing Na^+ ions. In embracing bulk water with a dielectric relaxation time τ_r~9.4 ps ($=1/(2\pi f_{cw})$) at 20 °C, the adenosine portion has a constrained water shell with τ_r~23 ps ($=1/(2\pi f_{c2})$), whereas the phosphoryl groups are surrounded by a constrained water layer with τ_r ~23 ps together with a three to four layers of hyper-mobile water with τ_r~8.4 ps ($=1/(2\pi f_{c1})$).

(unpublished). In the earlier experimental studies of solutions of these salts, the hydration effects of K^+ and Cl^-have been assumed to be the same in KCl solutions [27–29]. From the DR measurements of aqueous solutions on NaX (X, halide ions) alone, however, it is impossible to estimate the DR parameters for the anion and cation separately in solution.

Nonetheless, the total number of water molecules affected by Na^+ and Cl^- pairs is only 28 [13]. Even if the hydration layers of Na^+ and Cl^- had the same DR properties, both the number of constrained waters and the HMW found in solutions of Pi and adenine nucleotides could be attributed mostly to HPO_4^{2-} or AMP^{2-}, ADP^{3-}, and ATP^{4-}, rather than to Na^+.

Comparing the hydration properties of AMP with Pi (AMP can be regarded as a phosphoryl moiety, one hydrogen atom of which is replaced by an adenosine moiety), the increased portion of constrained water was equivalent to that of adenosine, and the HMW number was almost equal to that of Pi. Thus, the hydration increase from AMP to ADP and from ADP to ATP reflects the increase in the phosphoryl group number.

3.8. On assignment of low frequency relaxation components ranged from 0.2 to 2 GHz

In the case of adenosine solution with no counter ions in the pH range measured, f_{c3} (~0.9 GHz) may correspond to the rate of reorientation motion of an adenosine molecule or a part of it just like the reorientation frequencies of amino acids in water [8,30]. For adenosine phosphates, if f_{c3} indicates the reorientation rate of solute molecules, it should decrease with the increasing number of phosphoryl groups due to the viscous force. Although f_{c3} seems constant irrespective to the number of phosphoryl groups, its accompanying errors were relatively too large to make a clear assignment of the mode. However, it is not unlikely that the low frequency component ~0.3 GHz is a mixed mode of molecular reorientation and counter ionic cloud motion around phosphoryl groups.

3.9. Hydration states of adenine nucleotides and ATP hydrolysis

In order to discuss the implications of hydration states of adenine nucleotides revealed by the present study in thermodynamics of ATP hydrolysis, Fig. 5 shows a thermodynamic cycle of a hypothetical reaction A→B. In the case of ATP hydrolysis, A and B correspond to ATP + H_2O and ADP + Pi, respectively. On the basis of a wide range of experimental data, Alberty and Goldberg [31] formulated a method for the calculation of the thermodynamic parameters accompanying ATP hydrolysis in aqueous phase, which corresponds to step (1) in Fig. 5, as a function of pH.

For a closed thermodynamic cycle like the one in Fig. 5, the sum of the Gibbs energy changes accompanying the constituent steps (ΔG_i) is zero. Hence,

$$\Delta G_1 = \Delta G_2 + \Delta G_3 + \Delta G_4, \tag{7}$$

where ΔG_2 and ΔG_4 are the Gibbs energy changes of dehydration of reactants and hydration of products, respectively, and ΔG_3 is the Gibbs energy change for the reaction in the gas phase. ΔG_3 has now been rather accurately evaluated by an advanced quantum chemical method that takes into account the intramolecular effects such as the electrostatic repulsion and the opposing resonance effect [32]. Thus, if ΔG_2 and ΔG_4 were evaluated, it would be possible to check the thermodynamic consistency of calculations along the whole reaction cycle using Eq. (7).

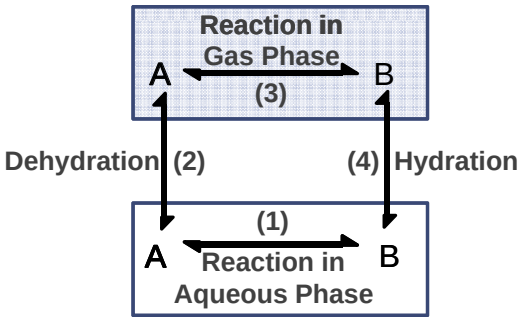

Fig. 5. Thermodynamic cycle of a hypothetical reaction A→B in aqueous phase. Step 1 is the reaction occurring in aqueous phase. At step 2, the reactant A is transferred into a gas phase, where A is allowed to change into B (step 3). At step 4, the product B is transferred back into the aqueous phase, followed by the reversal of step 1 that makes the whole system return to the initial state. There is no net energetic change by completion of this closed cycle. Hence, the Gibbs energy change for step 1 can be given by Eq. (7).

There have been several attempts to calculate ΔG_2 and ΔG_4 using QM/MM with Free Energy Perturbation (FEP) methods or Polarized Continuum Models (PCMs) etc. [4–7]. It should be noted that in the process of hydration or dehydration of any solute, not only is the structure of the solute molecules deformed by the surrounding water molecules (hydration effect) but also the structure and properties of the solvent water itself are perturbed. However, because of the inherent difficulty in carrying out the calculations with the large number of atoms involved, the effects caused by solute–solvent interactions have yet to be attempted.

Thus, in order to deepen a molecular understanding of the large negative $\Delta_{hyd}G$ associated with ATP hydrolysis, it is necessary to clarify the electronic structures of solute ions and to evaluate the contribution of ion-induced modulation of water structure to observed thermodynamic quantities. Our present results provide a detailed description of the perturbed solvent water states (constrained and hyper-mobile) around the reaction components of ATP hydrolysis. This will give deeper insight into solute–solvent interactions in the reaction system, which is invaluable to verify theoretical calculations and create models for theoretical consideration.

4. Conclusions

Hydration properties of adenine nucleotides and orthophosphate (Pi) in water have been revealed by high-resolution microwave dielectric relaxation (DR) analyses. Sample solutions were adjusted to pH = 8 with NaOH, so that the major ionic species of these solutions were AMP^{2-}, ADP^{3-}, ATP^{4-}, and HPO_4^{2-}, respectively. For comparison, the hydration of adenosine was also examined. The dielectric spectra were analyzed using a mixture theory combined with a least-squares Debye decomposition method. Solutions of Pi and adenine nucleotides showed qualitatively similar dielectric properties described by two Debye components. One component was characterized by a relaxation frequency (f_c = 18.8–19.7 GHz) significantly higher than that of bulk water (17 GHz) and the other by a much lower f_c (6.4–7.6 GHz), which are referred to as hyper-mobile water and constrained water, respectively. By contrast, a hydration shell of only the latter type was found for adenosine (f_c ~ 6.7 GHz). With increasing numbers of phosphoryl groups attached to the adenosine moiety, the number of water molecules increased both in hyper-mobile and constrained components. Based on our earlier DR study on the hydration of sodium halide salts [13], the contribution of co-increasing Na^+ concentration to the overall dielectric properties of Pi, and adenine nucleotides solutions could not be quantitatively significant. Thus, the present results indicate that phosphoryl groups are mostly responsible for affecting the structure of water surrounding adenine nucleotides by forming one constrained water layer and an additional three or four layers of hyper-mobile water.

Acknowledgment

We thank T. Miyazaki (Tohoku Univ.) for the discussion and support and D. M. Standley (Osaka Univ.) for reading the manuscript. This study was supported in part by grants from the Scientific Research on Innovative Areas, Ministry of Education, Culture, Sports, Science and Technology, Japan (18031004, 20118001, 20118008), and Core Research of Evolutional Science and Technology of Japan Science and Technology Agency.

Appendix A. Supplementary data

Supplementary data to this article can be found online at doi:10.1016/j.bpc.2010.11.006.

References

[1] F. Lipmann, Metabolic generation and utilization of phosphate bond energy, Adv. Enzymol. 1 (1941) 99–162.
[2] D. Voet, J.G. Voet, Biochemistry, third edition, John Wiley and Sons, Inc, Hoboken, NJ, 2004, pp. 566–571.
[3] P. George, R.J. Witonsky, M. Trachtman, C. Wu, W. Dorwart, L. Richman, W. Richman, F. Shurayh, B. Lentz, 'Squiggle-H_2O' an enquiry into the importance of solvation effects in phosphate ester and anhydride reactions, Biochim. Biophys. Acta 223 (1970) 1–15.
[4] D.M. Hayes, G.L. Kenyon, P.A. Kollman, Theoretical calculations of the hydrolysis energies of some 'high-energy' molecules. 2. A survey of some biologically important hydrolytic reactions, J. Am. Chem. Soc. 100 (1978) 4331–4340.
[5] M.E. Colvin, E. Evleth, Y. Akacem, Quantum chemical studies of pyrophosphate hydrolysis, J. Am. Chem. Soc. 117 (1995) 4357–4362.
[6] Y.N. Wang, I.A. Topol, J.R. Collins, S.K. Burt, Theoretical studies on the hydrolysis of mono-phosphate and tri-phosphate in gas phase and aqueous solution, J. Am. Chem. Soc. 125 (2003) 13265–13273.
[7] S.C.L. Kamerlin, A. Warshel, On the energetics of ATP hydrolysis in solution, J. Phys. Chem. B 113 (2009) 15692–15698.
[8] M. Suzuki, J. Shigematsu, Y. Fukunishi, T. Kodama, Hydrophobic hydration analysis on amino acid solutions by the microwave dielectric method, J. Phys. Chem. B 101 (1997) 3839–3845.
[9] M. Suzuki, J. Shigematsu, Y. Fukunishi, Y. Harada, T. Yanagida, T. Kodama, Coupling of protein surface hydrophobicity change to ATP hydrolysis by myosin motor domain, Biophys. J. 72 (1997) 18–23.
[10] S.R. Kabir, K. Yokoyama, K. Mihashi, T. Kodama, M. Suzuki, Hyper-mobile water is induced around actin filaments, Biophys. J. 85 (2003) 3154–3161.
[11] M. Suzuki, S.R. Kabir, M.S.P. Siddique, U.S. Nazia, T. Miyazaki, T. Kodama, Myosin-induced volume increase of the hyper-mobile water surrounding actin filaments, Biochem. Biophys. Res. Commun. 322 (2004) 340–346.
[12] T. Kamei, M. Oobatake, M. Suzuki, Hydration of apomyoglobin in native, molten globule, and unfolded states by using microwave dielectric spectroscopy, Biophys. J. 82 (2002) 418–425.
[13] T. Miyazaki, T. Wazawa, G. Mogami, T. Kodama, M. Suzuki, Measurement of the dielectric relaxation property of water–ion loose complex in aqueous solutions of salt at low concentrations, J. Phys. Chem. A 112 (2008) 10801–10806.
[14] T. Wazawa, T. Miyazaki, Y. Sambongi, M. Suzuki, Hydration analysis of *Pseudomonas aeruginosa* cytochrome *c*551 upon acid unfolding by dielectric relaxation spectroscopy, Biophys. Chem. 151 (2010) 160–169.
[15] H. Sigel, R. Griesser, Nucleoside 5′-triphosphates: self-association, acid-base, and metal ion-binding properties in solution, Chem. Soc. Rev. 34 (2005) 875–900.
[16] T. Sato, A. Chiba, R. Nozaki, Dielectric relaxation mechanism and dynamical structures of the alcohol/water mixtures, J. Mol. Liq. 101 (2002) 99–111.
[17] T. Sato, R. Buchner, Cooperative and molecular dynamics of alcohol/water mixtures: the view of dielectric spectroscopy, J. Mol. Liq. 117 (2005) 23–31.
[18] T. Hanai, Theory of the dielectric dispersion due to interfacial polarization and its application to emulsions, Kolloid Z. 171 (1960) 23–31.
[19] R. Buchner, J. Barthel, J. Stauber, The dielectric relaxation of water between 0 °C and 35 °C, Chem. Phys. Lett. 306 (1999) 57–63.
[20] U. Kaatze, Complex permittivity of water as a function of frequency and temperature, J. Chem. Eng. Data 34 (1989) 371–374.
[21] R. Pethig, Dielectric and electronic properties of biological materials, John Wiley and Sons, Inc, 1979, pp. 1–69., Chichester, New York, Brisbane, Toronto.
[22] K.W. Wagner, Erklärung der dielektrischen Nach wirkungsvorgänge auf Grund Maxwellscher Vorstellungen, Arch. Elektrotech. 2 (1914) 371–387.
[23] M. Kinoshita, M. Suzuki, A statistical–mechanical analysis on the hyper-mobile water around a large solute with high surface charge density, J. Chem. Phys. 130 (2009) 14707, (1–11).
[24] J.-C. Liao, S. Sun, D. Chandler, G. Oster, The conformational states of Mg·ATP in water, Eur. Biophys. J. 33 (2004) 29–37.
[25] T. Yamaguchi, T. Matsuoka, S. Koda, Theoretical study on the sound absorption of electrolytic solutions. I. Theoretical formulation, J. Chem. Phys. 126 (2007) 144505.
[26] T. Chen, G. Hefter, R. Buchner, Dielectric spectroscopy of aqueous solutions of KCl and CsCl, J. Phys. Chem. A 107 (2003) 4025–4031.
[27] H.L. Friedman, C.V. Krishnan, in: F. Franks (Ed.), Water a Comprehensive Treatise, Vol. 3, Plenum Press, New York-London, 1973, pp. 47–53.
[28] Y. Marcus, Ion properties, Marcel Dekker, Inc, New York, NY, 1997, pp. 199–208.
[29] Y. Marcus, Effect of ions on the structure of water: structure making and breaking, Chem. Rev. 109 (2009) 1346–1370.
[30] R. Pethig, Dielectric and electronic properties of biological materials, John Wiley & Sons, New York, 1979, pp. 78–91.
[31] R.A. Alberty, R.N. Goldberg, Standard thermodynamic formation properties for the adenosine 5′-triphosphate series, Biochemistry 31 (1992) 10610–10615.
[32] P. Hansia, N. Guruprasad, S. Vishveshwara, Ab initio studies on the tri- and diphosphate fragments of adenosine triphosphate, Biophys. Chem. 119 (2006) 127–136.
[33] J.J. Christensen, J.H. Rytting, R.M. Izatt, Thermodynamic pK, ΔH° ΔS° and ΔCp° values for proton dissociation from several purines and their nucleosides in aqueous solution, Biochemistry 9 (1970) 4907–4913.